

# Single-Step and Multistep Mechanisms of Aromatic Nucleophilic Substitution of Halobenzenes and Halonitrobenzenes with Halide Anions: Ab Initio Computational Study

Mikhail N. Glukhovtsev,<sup>\*,1a,b</sup> Robert D. Bach,<sup>1b</sup> and Sergei Laiter<sup>1c</sup>

Department of Chemistry, Wayne State University, Detroit, Michigan 48202, Department of Chemistry and Biochemistry, University of Delaware, Newark, Delaware 19716, and Laboratory for Molecular Modeling, School of Pharmacy, University of North Carolina, Chapel Hill, North Carolina 27599

Received November 11, 1996<sup>®</sup>

The  $C_6H_5X + X^-$  ( $X = Cl-I$ ) gas phase  $S_NAr$  reactions proceed via a single-step mechanism without the formation of a stable  $C_6H_5X_2^-$   $\sigma$ -complex. The  $C_{2v}$  structures of  $C_6H_5X_2^-$  ( $X = Cl-I$ ), which are transition structures in these reactions, are predicted to be considerably higher in energy (by 102.3 (Cl), 100.3 (Br), and 103.7 (I)  $\text{kJ mol}^{-1}$  at the MP2/6-31+G(d) + ZPE(HF/6-31+G(d)) level) than their isolated reactants. These high overall barriers suggest that it would be hardly possible to observe the  $S_NAr$  reactions of monosubstituted halobenzenes with halide anions in the gas phase. The introduction of a nitro group into the benzene ring, however, leads to a significant decrease in the overall barrier and for 1-chloro-4-nitrobenzene (**5**) in its reaction with  $Cl^-$  the overall barrier is only 18.6  $\text{kJ mol}^{-1}$  (B3LYP/6-31+G(d) + ZPE(B3LYP/6-31+G(d))). This reaction also follows a concerted pathway without the formation of an intermediate. The stabilization energies for  $\sigma$ -complexes **8–10** formed in the reactions of 1-chloro-4-nitrobenzene (**5**), 1-chloro-2,4-dinitrobenzene (**6**), and picryl chloride (**7**) with chloride anion demonstrate that the introduction of the first nitro group leads to a stabilization energy of 94.1  $\text{kJ mol}^{-1}$  and the second and third nitro groups result in an additional stabilization by 70.0 and 128.9  $\text{kJ mol}^{-1}$ , respectively (at the B3LYP/6-31+G(d) + ZPE(B3LYP/6-31+G(d)) level). As a consequence, the gas phase reactions of 1-chloro-2,4-dinitrobenzene (**6**) and picryl chloride (**7**) with chloride anion follow a multistep mechanism with the formation of the  $\sigma$ -complexes **9** and **10** as intermediates. The  $C_6H_5F + F^-$   $S_NAr$  reaction proceeds via a multistep mechanism with the formation of a discrete  $C_6H_5F_2^-$   $\sigma$ -complex as an intermediate, the energy of which is 15.5  $\text{kJ mol}^{-1}$  lower than that of the separated reactants. The activation barrier for the elimination of the fluoride anion from this complex is 6.3  $\text{kJ mol}^{-1}$  at the MP2/6-31+G(d) + ZPE(HF/6-31+G(d)) levels. The negative overall barrier of  $-9.2 \text{ kJ mol}^{-1}$  for reaction (1) with  $X = F$  indicates that this reaction may be feasible in the gas phase provided that competing reactions do not dominate.

## 1. Introduction

Aromatic nucleophilic substitution ( $S_NAr$ ) reactions constitute an active field of organic chemistry, which is very important from the viewpoints of both practical applications<sup>2</sup> and the theory of nucleophilic reaction mechanisms.<sup>3</sup> Among a variety of suggested reaction mechanisms for such nucleophilic aromatic substitution,<sup>3–5</sup> the most commonly accepted reaction path is an ionic addition–elimination multistep mechanism ( $Ad_N-E$ ) which is initiated by nucleophilic attack at the  $\pi$ -aromatic

system (benzenoid or heteroaromatic).<sup>2,3</sup> Another category of reaction mechanism is comprised of multistep reaction pathways that can involve single electron transfer (SET) to the aromatic substrate, fragmentation of the forming radical anion to an aryl radical and ensuing chain, or nonchain reactions of the radical via the rather well-established  $S_{RN}1$  mechanism. A single-step  $S_{RN}2$  mechanism has also been suggested recently, but its feasibility is the subject of current debate.<sup>4,5</sup> The  $Ad_N-E$  mechanism involves the formation of a carbanionic intermediate or several such intermediates that can undergo intramolecular rearrangement via migration of the nucleophile or the leaving group. Such intermediates which may be stabilized, for example, by nitro groups, have been isolated and studied in detail (Meisenheimer complexes).<sup>3f,h,6</sup>

Although the *multistep* character of heterolytic pathways appears as an unquestionable explicit feature of  $S_NAr$  reactions,<sup>2b,3f–h</sup> experimental data indicating that

<sup>®</sup> Abstract published in *Advance ACS Abstracts*, May 15, 1997.

(1) (a) Wayne State University. E-mail: mng@udel.edu. WWW: <http://udel.edu/~mng/>. (b) University of Delaware. E-mail: rbach@udel.edu. WWW: <http://www.udel.edu/chem/bach>. (c) University of North Carolina.

(2) (a) *Comprehensive Organic Synthesis*; Trost, B., Ed.; Pergamon Press: New York, 1991; Vol. 4, Chapter 2. (b) Stock, L. M. *Aromatic Substitution Reactions*; Prentice-Hall: Englewood Cliffs, NJ, 1968. (c) Clark, J. H.; Wails, D.; Bastock, T. W. *Aromatic Fluorination*; CRC Press: Boca Raton, FL, 1996.

(3) (a) Bunnet, J. F.; Zahler, R. E. *Chem. Rev.* **1951**, *49*, 273. (b) Miller, J. In *Aromatic Nucleophilic Substitution*; Eaborn, C., Chapman, N. B., Eds.; Elsevier: Amsterdam, 1968. (c) Bernasconi, C. F. *Chimia* **1980**, *31*, 1. (d) Makosza, M.; Winiarski, J. *Acc. Chem. Res.* **1987**, *20*, 282. (e) Illuminati, G.; Stegel, F. *Adv. Heterocycl. Chem.* **1983**, *34*, 306. (f) Terrier, F. *Nucleophilic Aromatic Displacement—The Influence of the Nitro Group*; Feuer, H., Ed.; VCH Publishers: New York, 1991. (g) Chupakhin, O. N.; Charushin, V. N.; van der Plas, H. C. *Nucleophilic Aromatic Substitution of Hydrogen*; Academic Press: San Diego, 1994. (h) Knyazev, V. N.; Drozd, V. N. *Russ. J. Org. Chem.* **1995**, *31*, 1.

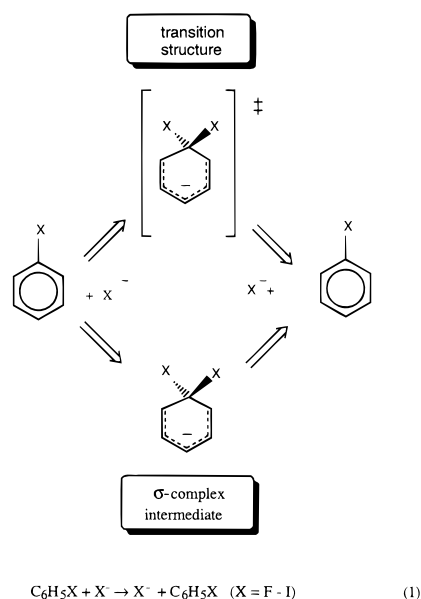
(4) (a) Bunnet, J. F. *Acc. Chem. Res.* **1978**, *11*, 413. (b) Bunnet, J. F. *Acc. Chem. Res.* **1992**, *25*, 2. (c) Bunnet, J. F. *Tetrahedron* **1993**, *49*, 4477.

(5) (a) Rossi, R. A.; de Rossi, R. H. *Aromatic Substitution by the  $S_{RN}1$  Mechanism*, Monograph 178; American Chemical Society: Washington, DC, 1983. (b) Norris, R. K. In *The Chemistry of Functional Groups*; Patai, S., Rappoport, Z., Eds.; Wiley: Chichester, U.K., 1983; Suppl. D, Chapter 16. (c) Bowman, W. R. *Chem. Soc. Rev.* **1988**, *17*, 283. (d) Savéant, J.-M. *Adv. Phys. Org. Chem.* **1990**, *26*, 1. (e) Denney, D. B.; Denney, D. Z. *Tetrahedron* **1991**, *47*, 6577. (f) Savéant, J.-M. *Tetrahedron* **1994**, *50*, 10117.

(6) (a) Terrier, F. *Chem. Rev.* **1982**, *82*, 78. (b) Crampton, M. R. In *Organic Reaction Mechanisms*; Knipe, A. C., Watts, W. E., Eds.; Wiley: New York, 1988; Chapter 7.

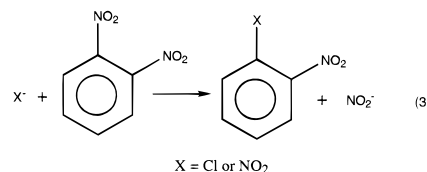
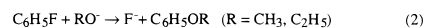
phenolate anions react with 2-(4-nitrophenoxy)-4,6-dimethoxy-1,3,5-triazine in aqueous solution via a *single-step* mechanism of nucleophilic aromatic substitution<sup>7</sup> presents a challenge to the conventional concept of S<sub>N</sub>Ar reactions. A single-step mechanism of the nucleophilic substitution at unsaturated carbon may be not so unusual as it was thought earlier. Recently it has been shown that the nucleophilic substitution at an unactivated vinyl carbon can proceed via a single-step mechanism<sup>8</sup> with inversion of configuration.<sup>8a</sup>

There have been few theoretical studies on the feasibility of the single-step versus multistep aromatic nucleophilic substitution. Semiempirical calculations using MNDO and AM1 methods showed that the gas phase reactions of halobenzenes with halide anions can involve a single-step mechanism.<sup>9,10</sup> For example, chlorobenzene with such nucleophiles as methoxide and hydride anions reacts via a single-step mechanism without the formation of intermediate anionic  $\sigma$ -complexes.<sup>9</sup>

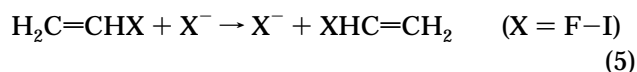


Few data have been accumulated for S<sub>N</sub>Ar reactions in the gas phase<sup>11-14</sup> since they are often accompanied by various competitive reactions such as proton transfer, elimination, or S<sub>N</sub>2 reaction at a carbon atom in the substituent.<sup>12,14</sup> Methoxide and ethoxide anions were found<sup>11a</sup> to react slowly with fluorobenzenes leading to the displacement of fluoride anion (eq 2). The formation

of a Meisenheimer-type intermediate was postulated for these reactions.<sup>11a</sup> The presumption that these gas phase nucleophilic substitution reactions occur via a Meisenheimer-type complex was supported by the interpretation of the data on the gas phase reactions of dinitrobenzenes (eq 3) where a [C<sub>6</sub>H<sub>4</sub>(NO<sub>2</sub>)<sub>2</sub>]Cl<sup>-</sup> ion was observed.<sup>11b</sup> The structure of this ion, however, has not been established. In fact, the mechanism of gas phase aromatic nucleophilic substitution has not been firmly established by either experimental or theoretical studies and many key questions remain open.



In the present work we consider single-step and multistep mechanisms of gas phase S<sub>N</sub>Ar reactions using the results of ab initio calculations on the identity halide-exchange reaction (eq 1) for the entire set of halide anions, from fluoride to iodide. Reactions of this type in solution, which exemplify an archetype of S<sub>N</sub>Ar reaction, have been studied well.<sup>15</sup> How does the nature of the nucleophile affect the reaction mechanism? It has been suggested that gas phase S<sub>N</sub>Ar substitutions do not necessarily require activation of the aromatic system by electron-withdrawing substituents.<sup>6f</sup> We also address the effect of such substituents on the gas phase S<sub>N</sub>Ar reaction mechanism. Could such electron-withdrawing substituents as nitro groups considerably decrease the barrier heights of gas phase S<sub>N</sub>Ar reactions and make these reactions feasible? Are these substituents capable of changing the reaction mechanism from single-step to multistep processes? In this study we also compare the gas phase S<sub>N</sub>Ar reactions (1) with gas phase nucleophilic substitution reactions at saturated (eq 4) and vinyl carbons (eq 5).



## 2. Computational Methods

Ab initio molecular orbital calculations<sup>16</sup> were carried out with the GAUSSIAN-92/DFT and GAUSSIAN-94 systems of programs.<sup>17</sup> For bromine- and iodine-containing species, the quasi-relativistic energy-adjusted spin-orbit-averaged seven-valence electron effective core potentials (ECP) developed by the Stuttgart group,<sup>18</sup> were used. The [31,31] valence basis sets for bromine and iodine were augmented by polarization d functions and by diffuse s and p functions.<sup>19</sup> The all-electron 6-31+G(d) basis set was employed for carbon, hydrogen, fluorine, and chlorine. We loosely refer to our calculations on reaction (1) as carried out with the 6-31+G(d) basis set. The Becke's three-parameter hybrid functional<sup>20a</sup> combined with

(7) Renfrew, A. H.; Taylor, J. A.; Whitmore, J. M. J.; Williams, A. *J. Chem. Soc., Perkin Trans. 2* **1993**, 1703.

(8) (a) Glukhovtsev, M. N.; Pross, A.; Radom, L. *J. Am. Chem. Soc.* **1994**, *116*, 5961. (b) Bach, R. D.; Wolber, G. *J. Am. Chem. Soc.* **1984**, *106*, 1401.

(9) (a) Gluz, E. B.; Glukhovtsev, M. N.; Simkin, B. Ya.; Minkin, V. I. *Russ. J. Org. Chem. (Engl. Transl.)* **1992**, *28*, 499. (b) Gluz, E. B.; Glukhovtsev, M. N.; Simkin, B. Ya.; Minkin, V. I. *Russ. J. Org. Chem. (Engl. Transl.)* **1992**, *28*, 1439. (c) Simkin, B. Ya.; Gluz, E. B.; Glukhovtsev, M. N.; Minkin, V. I. *J. Mol. Struct. (Theochem)* **1993**, *284*, 123.

(10) (a) Dotterer, S. K.; Harris, R. L. *J. Org. Chem.* **1988**, *53*, 777. (b) Yamabe, S.; Minato, T.; Kawabata, Y. *Can. J. Chem.* **1984**, *62*, 235.

(11) (a) Briscese, S. M. J.; Riveros, J. M. *J. Am. Chem. Soc.* **1975**, *97*, 230. (b) Bowie, J. H.; Stapleton, B. J. *Aust. J. Chem.* **1977**, *30*, 795.

(12) (a) Ingemann, S.; Nibbering, N. M. M. *J. Org. Chem.* **1983**, *48*, 183. (b) Ingemann, S.; Nibbering, N. M. M. *Nouv. J. Chim.* **1984**, *8*, 299.

(13) Linnert, H. V.; Riveros, J. M. *Int. J. Mass Spectrom. Ion Process.* **1994**, *140*, 163.

(14) Riveros, J. M.; Jose, S. M.; Takashima, K. *Adv. Phys. Org. Chem.* **1985**, *21*, 197.

(15) (a) Fluoride exchanges, e.g.: Terrier, F.; Ah-Kow, C.; Pouet, M. J.; Simonnin, M. P. *Tetrahedron Lett.* **1976**, 227. (b) Chloride exchanges, e.g.: Gore, P. H.; Hundal, A. S.; Morris, D. F. C. *Tetrahedron* **1981**, *37*, 167. (c) Bromide exchanges, e.g.: Sharan, M. *Indian J. Chem.* **1969**, *7*, 465. (d) Iodide exchanges, e.g.: Kendall, F. H.; Miller, J. J. *Chem. Soc. B* **1967**, 119.

(16) Hehre, W. J.; Radom, L.; Schleyer, P. v. R.; Pople, J. A. *Ab Initio Molecular Orbital Theory*; Wiley: New York, 1986.

the Lee, Yang, and Parr (LYP) correlation functional,<sup>20b</sup> denoted B3LYP,<sup>20c</sup> was employed in the calculations using density functional theory (DFT). Geometries were optimized using analytic gradient techniques.<sup>21</sup> The stationary points on the potential energy surfaces were characterized by calculations of vibrational frequencies, which were done analytically for the species containing the first- and second-row atoms and numerically for ECP calculations of bromine- and iodine-containing species at the HF and DFT levels.<sup>22</sup> The zero-point vibrational energies (ZPE) calculated at the HF level were scaled by 0.9135.<sup>23</sup> The scaling factor for the B3LYP/6-31+G(d) calculated zero-point energies is 0.98.<sup>24</sup> The frozen-core approximation was used in the MP2 calculations. Temperature corrections to enthalpy were calculated using the HF/6-31+G(d) or B3LYP/6-31+G(d) frequencies, respectively, and standard formulas of statistical thermodynamics.<sup>15</sup> Throughout this paper, relative energies are presented as enthalpy changes ( $\Delta H$ ) at 0 K (including ZPE(HF/6-31+G(d)) or ZPE(B3LYP/6-31+G(d))), bond lengths are in angstroms, and bond angles are in degrees. The MP2/6-31+G(d) + ZPE(HF/6-31+G(d)) and B3LYP/6-31+G(d) + ZPE(B3LYP/6-31+G(d)) levels of theory are the highest levels used in our calculations on reaction (1) and the  $S_NAr$  reactions of nitrobenzenes. At present these computational levels are the highest ones which have been applied for studying aromatic nucleophilic substitution reactions.

A large number of calculations on  $S_N2$  reactions at saturated carbon have shown that the magnitudes of these reaction barriers are very sensitive to the level of theory employed.<sup>25–27</sup> Since these  $S_N2$  reactions are somewhat similar to the  $S_NAr$  reactions discussed herein, we have assessed the accuracy of the calculations at the MP2/6-31+G(d) and B3LYP/6-31+G(d) levels by carrying out calculations for the  $CH_3Cl + Cl^-$   $S_N2$  reaction and comparing these results with the data of higher level calculations and experimental data<sup>28–30</sup> on the energies of ion–molecule complexes and barrier heights for this  $S_N2$  reaction. Inspection of these results<sup>31</sup> shows that the complexation energy values ( $\Delta H_{comp}^\ddagger$ ) are not sensitive to the level of theory. However, the overall and central barriers (these

are the barrier relative to the isolated reactants,  $\Delta H_{ovr}^\ddagger$ , and the barrier relative to the ion–molecule complex,  $\Delta H_{cent}^\ddagger$ , respectively) are overestimated at the MP2/6-31+G(d) + ZPE-(HF/6-31+G(d)) level. In contrast, the overall and central barriers are underestimated at the B3LYP/6-31+G(d) + ZPE-(B3LYP/6-31+G(d)) level<sup>31</sup> as compared with the experimental values.<sup>28–30</sup> As shown recently,<sup>32</sup> halide anions are described correctly using DFT calculations. The basis set extension does not bring any significant improvement at the B3LYP level. Not surprisingly, the best results have been obtained using G2(+) theory.<sup>25</sup> However, application of G2 theory (and its modification, G2(+),<sup>25</sup> for calculations of anions) which corresponds effectively to calculations at the QCISD(T)/6-311+G(3df,2p) level with zero-point vibrational energy (ZPE) and higher level corrections,<sup>33</sup> for calculations on reaction (1) would be extremely computer time demanding and far beyond current normal computational capacity.

Thus, we could expect that reliable estimates of the complexation energies can be obtained from our calculations of reactions (1) at the MP2/6-31+G(d) + ZPE(HF/6-31+G(d)) and B3LYP/6-31+G(d) + ZPE(B3LYP/6-31+G(d)) levels of theory. Of course, the  $S_N2$  reactions (eq 4) at saturated carbon and the  $S_NAr$  reactions (1) are not completely analogous to each other. If the data on the  $S_N2$  reaction (eq 4) ( $X = Cl$ )<sup>31</sup> are used for predicting the performance of the same computational methods for  $S_NAr$  reactions (eq 1), one could expect that the calculations of reaction (1) at the MP2 level would result in considerably higher barriers when compared with those calculated using the B3LYP functional. It is gratifying that we have found the overall and central barriers (102.3 and 151.2 kJ mol<sup>-1</sup>) for the  $C_6H_5Cl + Cl^-$  reaction calculated at the MP2/6-31+G(d) + ZPE(HF/6-31+G(d)) level to agree quite well with the barriers calculated at the B3LYP/6-31+G(d) + ZPE-(B3LYP/6-31+G(d)) level (112.8 and 152.3 kJ mol<sup>-1</sup>). The energy of the formation of the prereaction complex, the overall and central barriers for the  $C_6H_5F + F^-$  reaction as well as the overall barriers for the  $C_6H_5Br + Br^-$  and  $C_6H_5I + I^-$   $S_NAr$  reactions calculated at the MP2 and B3LYP computational levels, respectively, are also close each other (see below). The computational data for the  $S_N2$  reaction (4) obtained at the same levels of theory do not show such good agreement.<sup>31</sup>

### 3. Results and Discussion

For the gas phase reactions of nucleophiles with aromatic molecules, various mechanisms of nucleophilic aromatic substitution compete with other reactions such as proton transfer,  $S_N2$  substitution, and E2-type elimination. In some cases the aromatic substitution reaction is not the dominant process.<sup>12–14</sup> In the present study we do not consider the possibility of proton transfer from the halobenzene to the attacking nucleophile<sup>9,10,12,13</sup> or

(17) (a) Frisch, M. J.; Trucks, G. W.; Head-Gordon, M.; Gill, P. M. W.; Wong, M. W.; Foresman, G. B.; Johnson, B. G.; Schlegel, H. B.; Robb, M. A.; Replogle, E. S.; Gomperts, R.; Andres, J. L.; Raghavachari, K.; Binkley, J. S.; Gonzalez, C.; Martin, R. L.; Fox, D. J.; DeFrees, D. J.; Baker, J.; Stewart, J. J. P.; Pople, J. A. GAUSSIAN 92/DFT, Revision F. 2., Gaussian Inc., Pittsburgh, PA, 1993. (b) Frisch, M. J.; Trucks, G. W.; Schlegel, H. B.; Gill, P. M. W.; Johnson, B. G.; Robb, M. A.; Cheeseman, J. R.; Keith, T. A.; Peterson, G. A.; Montgomery, J. A.; Raghavachari, K.; Al-laham, M. A.; Zakrzewski, V. G.; Ortiz, J. V.; Foresman, J. B.; Cioslowski, J.; Stefanov, B. B.; Nanayakkara, A.; Challacombe, M.; Peng, C. Y.; Ayala, P. Y.; Wong, M. W.; Replogle, E. S.; Gomperts, R.; Andres, J. L.; Martin, R. L.; Fox, D. J.; Binkley, J. S.; DeFrees, D. J.; Baker, J.; Stewart, J. J. P.; Head-Gordon, M.; Gonzalez, C.; Pople, J. A. GAUSSIAN-94, Gaussian Inc., Pittsburgh, PA, 1995.

(18) Bergner, A.; Dolg, M.; Küchle, W.; Stoll, H.; Preuss, H. *Mol. Phys.* **1993**, *80*, 1431.

(19) Glukhovtsev, M. N.; Pross, A.; McGrath, M. P.; Radom, L. *J. Chem. Phys.* **1995**, *103*, 1878.

(20) (a) Becke, A. D. *J. Chem. Phys.* **1993**, *98*, 5648. (b) Lee, C.; Yang, W.; Parr, R. G. *Phys. Rev. B* **1988**, *37*, 785. (c) Stephens, P. J.; Devlin, F. J.; Chabalowski, C. F.; Frisch, M. J. *J. Phys. Chem.* **1994**, *98*, 11623.

(21) (a) Schlegel, H. B. *J. Comput. Chem.* **1982**, *3*, 214. (b) Schlegel, H. B. In *Ab Initio Methods in Quantum Chemistry*; Lawley, K. P., Ed.; Wiley: New York, 1987; p 249. (c) Schlegel, H. B. In *Modern Electronic Structure Theory*; Yarkony, D. R., Ed.; World Scientific: Singapore, 1995; p 459.

(22) Handy, N. C.; Tozer, D. J.; Laming, G. J.; Murray, C. W.; Amos, R. D. *Israel J. Chem.* **1993**, *33*, 331.

(23) Pople, J. A.; Scott, A. P.; Wong, M. W.; Radom, L. *Israel J. Chem.* **1993**, *33*, 345.

(24) Bauschlicher, C. W.; Partridge, H. *Chem. Phys. Lett.* **1995**, *240*, 533.

(25) (a) Glukhovtsev, M. N.; Pross, A.; Radom, L. *J. Am. Chem. Soc.* **1995**, *117*, 2024. (b) Glukhovtsev, M. N.; Pross, A.; Radom, L. *J. Am. Chem. Soc.* **1995**, *117*, 9012. (c) Glukhovtsev, M. N.; Pross, A.; Radom, L. *J. Am. Chem. Soc.* **1996**, *118*, 6273. (d) Glukhovtsev, M. N.; Schelegel, H. B.; Pross, A.; Radom, L.; Bach, R. D. *J. Am. Chem. Soc.* **1996**, *118*, 11258.

(26) Shaik, S. S.; Schlegel, H. B.; Wolfe, S. *Theoretical Aspects of Physical Organic Chemistry. The  $S_N2$  Mechanism*; Wiley: New York, 1992.

(27) (a) Basilevsky, M. V.; Koldobskii, S. G.; Tikhomirov, V. A. *Russ. Chem. Rev. (Engl. Transl.)* **1986**, *55*, 948. (b) Cernusak, I.; Urban, M. *Collect. Czech. Chem. Commun.* **1988**, *53*, 2239. (c) Shi, Z.; Boyd, R. J. *J. Am. Chem. Soc.* **1989**, *111*, 1575. (d) Shi, Z.; Boyd, R. J. *J. Am. Chem. Soc.* **1990**, *112*, 6789. (e) Vande Linde, S. R.; Hase, W. L. *J. Phys. Chem.* **1990**, *94*, 2778. (f) Vande Linde, S. R.; Hase, W. L. *J. Phys. Chem.* **1990**, *94*, 6148. (g) Wolfe, S.; Kim, C.-K. *J. Am. Chem. Soc.* **1991**, *113*, 8056. (h) Zhao, X. G.; Tucker, S. C.; Truhlar, D. G. *J. Am. Chem. Soc.* **1991**, *113*, 826. (i) Boyd, R. J.; Kim, C.-K.; Shi, Z.; Weinberg, N.; Wolfe, S. *J. Am. Chem. Soc.* **1993**, *115*, 10147. (j) Wladkowski, B. D.; Allen, W. D.; Brauman, J. I. *J. Phys. Chem.* **1994**, *98*, 13532. (k) Deng, L.; Branchadell, V.; Ziegler, T. *J. Am. Chem. Soc.* **1994**, *116*, 10645.

(28) Larson, J. W.; McMahon, T. B. *J. Am. Chem. Soc.* **1984**, *106*, 517.

(29) Barlow, S. E.; Van Doren, J. M.; Bierbaum, V. M. *J. Am. Chem. Soc.* **1988**, *110*, 7240.

(30) Wladkowski, B. D.; Brauman, J. I. *J. Phys. Chem.* **1993**, *97*, 13158.

(31) For a detailed study of the B3LYP performance in calculations of  $S_N2$  reactions at saturated carbon, see: Glukhovtsev, M. N.; Bach, R. D.; Pross, A.; Radom, L. *Chem. Phys. Lett.* **1996**, *260*, 558.

(32) Galbraith, J. M.; Schaefer, H. F. *J. Chem. Phys.* **1996**, *105*, 862.

(33) Curtiss, L. A.; Raghavachari, K.; Trucks, G. W.; Pople, J. A. *J. Chem. Phys.* **1991**, *94*, 7221.

**Table 1. Complexation Energy and Barrier Heights for the S<sub>N</sub>Ar Reaction of Halobenzenes with Halide Anions (eq 1) Calculated at Various Computational Levels (in kJ mol<sup>-1</sup>)<sup>a</sup>**

	computational level	$\Delta H_{\text{comp}}$	$\Delta H_{\text{ovr}}^{\ddagger}$	$\Delta H_{\text{cent}}^{\ddagger}$
X = F	MP2/6-31+G(d)	71.1	-9.2 <sup>b</sup>	61.9 <sup>b</sup>
X = F	B3LYP/6-31+G(d)	74.6	-15.6 <sup>c</sup>	59.0 <sup>c</sup>
X = Cl	MP2/6-31+G(d)	48.9 <sup>d</sup>	102.3	151.2 <sup>e</sup>
X = Cl	B3LYP/6-31+G(d)	39.5 <sup>f</sup>	112.7	152.2 <sup>e</sup>
X = Br	MP2/6-31+G(d)	44.2	100.3	144.5 <sup>e</sup>
X = Br	B3LYP/6-31+G(d)		111.3	
X = I	MP2/6-31+G(d)	38.4	103.7	142.1 <sup>e</sup>
X = I	B3LYP/6-31+G(d)		113.6	

<sup>a</sup> Total energies and zero-point energies are listed in Table 1S (Supporting Information). The relative energies include the ZPE(HF/6-31+G(d)) or ZPE(B3LYP/6-31+G(d)) corrections. <sup>b</sup> Relative energies are given for transition structure **4a**, see text. The relative energy of  $\sigma$ -complex **3a** with respect to the reactants and to loose ion-molecule complex **2a** are -15.5 and 55.6 kJ mol<sup>-1</sup>, respectively. The barrier for the isomerization of the  $\sigma$ -complex **3a** into the FC<sub>6</sub>H<sub>5</sub>...F<sup>-</sup> post-reaction ion-molecule complex is 6.3 kJ mol<sup>-1</sup>. <sup>c</sup> At the B3LYP/6-31+G(d) + ZPE(B3LYP/6-31+G(d)) level the relative energy of  $\sigma$ -complex **3a** with respect to the reactants is -26.8 kJ mol<sup>-1</sup>.  $\sigma$ -Complex **3a** is 47.8 kJ mol<sup>-1</sup> higher in energy than ion-molecule complex **2a** at this level of theory. <sup>d</sup> Experimental estimates<sup>37</sup> of the complexation energy for C<sub>6</sub>H<sub>5</sub>Cl...Cl<sup>-</sup> are 57 ± 8 and 57 ± 4 kJ mol<sup>-1</sup>. <sup>e</sup>  $\Delta H_{\text{comp}}$  values are based upon presumption that loose ion-molecule complexes **2a-d** are prereaction complexes. However, as discussed in the text, it is possible that the isomerizations of these complexes into the transition structures proceed via other ion-molecule complexes lying close in energy to **2a-d**; see also ref 9. <sup>f</sup> Calculated  $\Delta H_{\text{comp}}$  = 39.1 kJ mol<sup>-1</sup> at 298 K.

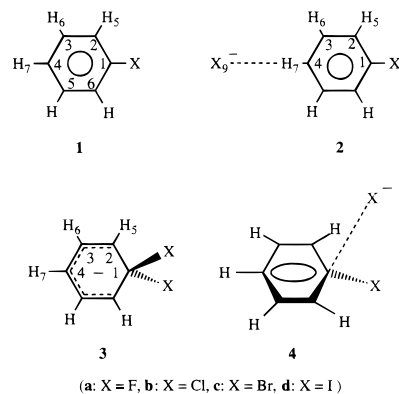
single electron transfer to the halobenzene.<sup>5,34</sup> Our attention will be focused on the ionic mechanisms of the aromatic nucleophilic substitution in order to determine whether S<sub>N</sub>Ar reactions (1) proceed via a multistep mechanism involving the formation of the intermediate  $\sigma$ -complex or whether such a complex represents a transition structure. As we found earlier,<sup>9</sup> the very first stage of the gas phase aromatic nucleophilic substitution reaction can be the formation of a loose ion-molecule prereaction complex. The formation of a long-lived ion-molecule complex has been found in a study of the gas phase aromatic nucleophilic reaction, F<sup>-</sup> + C<sub>6</sub>H<sub>5</sub>Cl, using Fourier transform ion cyclotron resonance spectroscopy.<sup>35</sup>

In a similar fashion to the notation used for the gas phase S<sub>N</sub>2 reactions at saturated carbon,<sup>25,30</sup> the energy of this ion-molecule complex with respect to the isolated reactants (i.e., complexation energy) is denoted as  $\Delta H_{\text{comp}}$ . The activation barriers relative to the reactants and to the prereaction ion-molecule complex are denoted as  $\Delta H_{\text{ovr}}^{\ddagger}$  and  $\Delta H_{\text{cent}}^{\ddagger}$ , respectively. If the  $\sigma$ -complex corresponds to a minimum,  $\Delta H_{\text{ovr}}$  and  $\Delta H_{\text{cent}}$  are notations for its energies relative to the reactants and to the ion-molecule complex. The calculated total energies of species involved in reactions (1) are given as Supporting Information (Table 1S). The complexation energies and reaction barriers are listed in Table 1.

**Reactants: Halobenzenes.** The geometries of halobenzenes optimized at the MP2/6-31+G(d) and B3LYP/6-31+G(d) levels as well as the experimental geometrical parameters are given in Table 2. The B3LYP and MP2 calculated geometries of halobenzenes are close each other. The C-X bond length optimized at the B3LYP/

6-31+G(d) level is on average slightly longer than the MP2/6-31+G(d) value for X = Cl-Br, but shorter for X = F (Table 2). In general, the optimized geometrical parameters agree well with the available experimental data.<sup>36</sup>

**Ion-Molecule Complexes.** As the charge-dipole interaction energy is maximal along the axis of the dipole moment, a geometry of the loose ion-molecule complex of the halobenzene with the attacking anion, in which the incoming anion lies in the plane of the benzene ring, is expected. Similar planar ion-molecule complexes have been found for gas phase nucleophilic substitution at vinylic carbon.<sup>8a</sup> The potential energy surface (PES) in the region close to these complexes should be rather flat. A planar structure of the F<sup>-</sup>...C<sub>6</sub>H<sub>5</sub>F ion-molecule complex **2a** is predicted to be a minimum at the HF/6-31+G(d) and B3LYP/6-31+G(d) levels of theory (the lowest frequency is 45 and 55 cm<sup>-1</sup>, respectively). The calculations for the X<sup>-</sup>...C<sub>6</sub>H<sub>5</sub>X (X = Cl-I) ion-molecule complexes **2b-d** yield one imaginary frequency with very small absolute values (6.5i, 8.2i, and 8.5i cm<sup>-1</sup>, respectively). However, the calculations of **2b** at a correlated level (B3LYP/6-31+G(d)) indicate this complex to be a minimum (the lowest frequency (b<sub>2</sub>) is 27.8 cm<sup>-1</sup>). Our attempts to optimize geometries of the *meta*- or *ortho*-coordinated complexes as well as of the complexes with halide anion coordinated with the two hydrogens at the HF/6-31+G(d) level were not successful because of an extreme flatness of the PES.



The experimental data on the complexation energies for the X<sup>-</sup>...C<sub>6</sub>H<sub>5</sub>X complexes **2** are available only for Cl<sup>-</sup>...C<sub>6</sub>H<sub>5</sub>Cl (57 ± 8 kJ mol<sup>-1</sup>).<sup>37</sup> Our calculated complexation energy for **2b** (48.9 kJ mol<sup>-1</sup> at the MP2/6-31+G(d) level; Table 1) agrees well with this experimental estimate. The B3LYP calculations lead to a slightly smaller value of 39.5 kJ mol<sup>-1</sup> (39.1 kJ mol<sup>-1</sup> at 298 K). Complex **2a**, F<sup>-</sup>...H<sub>5</sub>C<sub>6</sub>F, has the largest complexation energy (71.1 and 74.6 kJ mol<sup>-1</sup> at the MP2/6-31+G(d) and B3LYP/6-31+G(d) levels, respectively), whereas the complexation energies for **2b-d** vary in a range of 10 kJ mol<sup>-1</sup>, from 48.9 (**2b**) to 38.4 (**2d**) kJ mol<sup>-1</sup>. The calculated complexation energies for the X<sup>-</sup>...H<sub>5</sub>C<sub>6</sub>X (X = F-I) complexes **2a-d** are close to that for the X<sup>-</sup>...H<sub>3</sub>CX (X = F-I) and X<sup>-</sup>...H<sub>2</sub>C=CHX (X = F-I) ion-molecule complexes formed in the gas phase reactions of methyl halide and vinyl halide, respectively, with halide anions (Figure 1).<sup>8a,25</sup> By analogy with the complexation ener-

(34) Chowdhury, S.; Kebarle, P. In *Structure, Reactivity and Thermochimistry of Ions*; Ausloos, P., Lias, S. G., Eds.; Reidel: Dordrecht, 1987; p 321.

(35) Van Orden, S. L.; Pope, R. M.; Buckner, S. W. *Org. Mass Spectrom.* **1991**, *26*, 1003.

(36) Harmony, M. D.; Laurie, V. W.; Kuczkowski, R. L.; Ramsay, D. A.; Lovas, F. J.; Lafferty, W. J.; Maki, A. G. *J. Phys. Chem. Ref. Data* **1979**, *8*, 619.

(37) Lias, S. G.; Bartmess, J. E.; Liebman, J. F.; Holmes, J. L.; Levin, R. D.; Mallard, W. G. *J. Phys. Chem. Ref. Data* **1988**, *17*, Suppl. 1.

**Table 2. Structures of Halobenzenes 1a–d Optimized at the MP2/6-31+G(d) and B3LYP/6-31+G(d) Computational Levels<sup>a</sup>**

	F (1a)	Cl (1b)	Br (1c)	I (1d)
C1X	1.369 (1.361) <sup>b</sup> [1.354] <sup>c</sup>	1.742 (1.762) <sup>b</sup> [1.722] <sup>c</sup>	1.908 (1.918) <sup>b</sup> [1.87] <sup>c</sup>	2.126 (2.132) <sup>b</sup> [2.08] <sup>c</sup>
C1C2	1.390 (1.390) [1.383]	1.397 (1.395) [1.390]	1.397 (1.396)	1.399 (1.397)
C2C3	1.399 (1.399) [1.395]	1.398 (1.398) [1.390]	1.399 (1.398)	1.399 (1.399)
C3C4	1.399 (1.399) [1.397]	1.399 (1.398) [1.398]	1.399 (1.397)	1.398 (1.397)
C2H5	1.087 (1.085) [1.081]	1.087 (1.085) [1.077]	1.087 (1.085)	1.087 (1.085)
C3H6	1.088 (1.087) [1.086]	1.088 (1.087) [1.079]	1.088 (1.087)	1.088 (1.087)
C4H7	1.087 (1.086) [1.080]	1.087 (1.087) [1.080]	1.088 (1.087)	1.088 (1.087)
∠C2C1X	118.5 (118.6)	119.4 (119.3) [119.9]	119.2 (119.3)	119.4 (119.4)
∠C3C2C1	118.0 (118.3) [117.9]	119.1 (119.0) [119.7]	118.8 (119.0)	119.0 (119.1)
∠C4C3C2	120.5 (120.5) [120.5]	120.5 (120.5) [120.2]	120.5 (120.5)	120.5 (120.5)
∠H5C2C1	119.9 (119.8) [120.0]	120.0 (120.1) [119.5]	120.4 (120.3)	120.7 (120.7)
∠H6C3C2	119.4 (119.4) [119.9]	119.3 (119.3) [119.6]	119.3 (119.3)	119.3 (119.3)
∠H7C4C3	120.0 (120.1)	120.2 (120.1) [120.0]	120.1 (120.1)	120.1 (120.1)

<sup>a</sup> For numbering of the atoms see structure **1** in text. <sup>b</sup> Geometrical parameters optimized at the B3LYP/6-31+G(d) level are given in parentheses. <sup>c</sup> The available experimental geometrical parameters given in brackets were taken from ref 36.

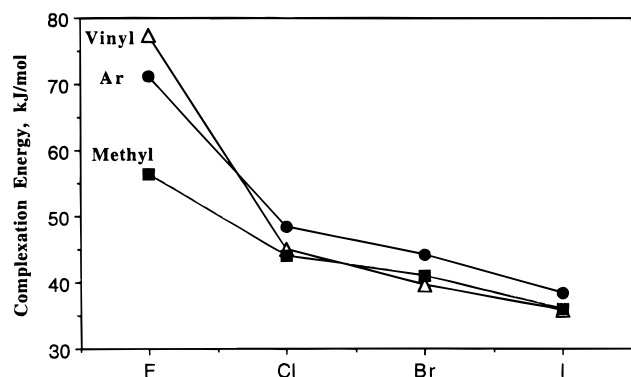


**Figure 1.** Complexation energies ( $\Delta H_{\text{comp}}$ ) of the ion–molecule complexes  $X^{\cdots}C_6H_5X$  ( $X = F-I$ ) (●) calculated at the MP2/6-31+G(d) + ZPE(HF/6-31+G(d)) level as well as the complexation energies of the  $Y^{\cdots}CH_3X$  (■) and of  $X^{\cdots}C_2H_3X$  (Δ) ( $X = F-I$ ) ion–molecule complexes, calculated at the G2(+)<sup>25a</sup> and G2(MP2)(+) levels, respectively. Complexation energies of the ion–molecule complexes  $X^{\cdots}C_6H_5X$  ( $X = F-I$ ) **2a–d** are listed in Table 1.

gies for the both methyl and vinyl halides,<sup>8a,25</sup> the complexation energies of **2a–d** demonstrate good linear correlations with the Mulliken ( $r^2 = 0.985$ ) and Pauling ( $r^2 = 0.993$ ) electronegativities<sup>38</sup> of halogens. Complexation of halobenzenes with halide anions lead to slight changes in the geometry of the  $C_6H_5X$  fragments (Table 2S given as Supporting Information).<sup>39</sup>

A theoretical study of nucleophilic aromatic substitu-

(38) For a discussion of the current status of the electronegativity concept in chemistry and for leading references, see: (a) Allen, L. C. *Int. J. Quant. Chem.* **1994**, *49*, 253. (b) Allen, L. C. *J. Am. Chem. Soc.* **1989**, *111*, 9003.

(39) The main changes are elongations of the C–H bond for the hydrogen atom coordinated with the incoming halide anion and of the C–X bond, respectively. The C–H bond elongations, the largest of which is 0.031 Å for complex **2a**, are proportional to the complexation energies. The  $X^{\cdots}H$  distances in the  $X^{\cdots}H_5C_6X$  complexes ( $X = F, Cl, \text{ and } Br$ ) are shorter than the upper boundary limits for specific interactions (2.24, 2.67, and 2.72 Å, respectively), estimated<sup>40</sup> from the mean-statistical values of the corresponding van der Waals radii (VWR) of the halogens and hydrogen,<sup>40d</sup> reflecting the bonding interaction between  $X^-$  and  $C_6H_5X$ . For  $X = I$ , the  $I^{\cdots}H$  distance in the complex **2d** is almost the same as the upper boundary limit for specific interactions (2.84 Å)<sup>40</sup> and this agrees with the smallest complexation energy for **2d** among the other  $X^{\cdots}H_5C_6X$  complexes. The changes in the geometry of the  $C_6H_5X$  fragment in **2**, which are caused by the complexation, are largest for  $X = F$ . While the C–H bond for the hydrogen coordinated with the incoming halide anion is only 0.006, 0.005, and 0.003 Å longer in **2b–d**, respectively, than that in corresponding halobenzenes **1b–d**, the C–H bond in **2a** (1.118 Å) is elongated by 0.031 Å as compared with the C–H bond in fluorobenzene calculated at the MP2/6-31+G(d) level (Table 2 and Table 2S). The halide complexation leads to a slight elongation of the C–X bond length in **2a–d** when compared with that in the halobenzenes.

tion using the MNDO method indicated the existence of local minima corresponding to charge transfer complexes between the arene and the incoming nucleophile, wherein the nucleophile was located above the arene ring.<sup>10a</sup> Our attempts to optimize the geometry of such a complex for  $F^-$  and  $C_6H_5F$  at the HF/6-31+G(d) level led to  $\sigma$ -complex **3a**. No charge transfer complex has been found in the MP2/6-31+G(d,p)//HF/6-31+G(d,p) calculations on the reaction of 1-chloro-2,4-dinitrobenzene with thiomethoxide anion, which have been published<sup>41</sup> since the present paper was submitted.

**$\sigma$ -Complexes: Transition Structures or Intermediates?** As noted above, we were not able to determine the minimal energy reaction pathway linking ion–molecule complex **2** and  $\sigma$ -complex **3** because of problems encountered in the geometry optimizations due to the extreme flatness of the PES near the isomeric structures of ion–molecule complexes. Therefore, while the previous MNDO and AM1 calculations<sup>8,9,25</sup> suggest that we may assign complexes **2** to the prereaction complexes, a detailed study of the reaction pathway is necessary for a definitive location of the prereaction ion–molecule complex. Thus, the structure of the prereaction ion–molecule complex in the  $S_NAr$  reaction (1) and the stabilization energies of these complexes still remain open questions. As the energies of various ion–molecule complexes appear to be close each other because of the weakness of their charge–dipole interactions, the energy of complex **2** can be used as an approximation to estimate the relative energy of  $\sigma$ -complex **3** with respect to the prereaction ion–molecule complex. This makes it possible to estimate the central barrier. However, we will concentrate our discussion mainly on the energies of  $\sigma$ -complexes **3** relative to the isolated reactants. What is important is that these energies rather than the energies with respect to the prereaction loose complex

(40) (a) Zefirov, Yu. V.; Zorkii, P. M. *Russ. Chem. Rev.* **1995**, *64*, 415 (Engl. Transl). (b) Zefirov, Yu. V.; Porai-Koshits, M. A. *Zh. Strukt. Khim.* **1980**, *21*, 150 (Engl. Transl). (c) Zefirov, Yu. V.; Porai-Koshits, M. A. *Zh. Strukt. Khim.* **1986**, *27*, 74 (Engl. Transl). (d) VWRs were obtained from X-ray diffraction data on organic crystal structures (VWR(H) = 1.16 Å, VWR(F) = 1.40 Å, VWR(Cl) = 1.90 Å, VWR(Br) = 1.97 Å, VWR(I) = 2.14 Å). Expression  $2\sqrt{R_A R_B}$  is used to estimate interatomic distances for ordinary van der Waals interactions using VWRs of A and B atoms, respectively.<sup>40a–c</sup> The upper limit for specific interactions is approximated as  $2\sqrt{R_A R_B} - 0.30$  Å.<sup>40c</sup>

(41) (a) Zheng, Y.-J.; Ornstein, R. L. *J. Am. Chem. Soc.* **1997**, *119*, 648. (b) Calculations at the MP2/6-31+G(d,p) level using the HF/6-31+G(d,p) geometries give rise to a qualitative change of the reaction profile when compared with the HF/6-31+G(d,p) results.<sup>41a</sup> It raises a question whether geometry optimizations at the HF level are reliable in the computational studies of  $S_NAr$  reactions.

**Table 3.** Structures ( $C_{2v}$ ) of  $\sigma$ -Complexes **3a–d** Optimized at the MP2/6-31+G(d) and B3LYP/6-31+G(d) Computational Levels<sup>a</sup>

	F ( <b>3a</b> )	Cl ( <b>3b</b> )	Br ( <b>3c</b> )	I ( <b>3d</b> )
C1X	1.498 (1.488) <sup>b</sup>	2.045 (2.131) <sup>b</sup>	2.279 (2.348) <sup>b</sup>	2.563 (2.642) <sup>b</sup>
C1C2	1.438 (1.449)	1.416 (1.411)	1.408 (1.403)	1.405 (1.398)
C2C3	1.393 (1.387)	1.395 (1.393)	1.397 (1.396)	1.398 (1.398)
C3C4	1.405 (1.405)	1.402 (1.403)	1.402 (1.401)	1.401 (1.400)
C2H5	1.089 (1.088)	1.087 (1.085)	1.087 (1.084)	1.087 (1.084)
C3H6	1.093 (1.092)	1.091 (1.090)	1.091 (1.090)	1.091 (1.089)
C4H7	1.089 (1.088)	1.089 (1.088)	1.089 (1.088)	1.089 (1.088)
$\angle$ XC1X	94.8 (95.4)	94.4 (93.3)	94.2 (93.6)	95.6 (95.1)
$\angle$ XC1C2	111.2 (111.1)	110.7 (110.3)	110.2 (109.9)	109.8 (109.4)
$\angle$ C2C1C6	115.5 (115.3)	117.2 (119.1)	119.0 (120.3)	119.5 (121.0)
$\angle$ C1C2C3	121.6 (121.4)	121.1 (119.9)	120.1 (119.3)	119.9 (119.0)
$\angle$ C4C3C2	122.0 (122.4)	121.4 (121.6)	121.1 (121.3)	121.1 (121.1)
$\angle$ C3C4C5	117.3 (117.1)	117.8 (118.0)	118.4 (118.4)	118.6 (118.8)
$\angle$ H5C2C3	121.1 (121.4)	120.3 (120.9)	119.4 (120.8)	119.9 (120.6)
$\angle$ H6C3C2	118.2 (118.3)	118.5 (118.5)	118.6 (118.6)	118.7 (118.8)
$\angle$ H7C4C3	121.4 (121.5)	121.1 (121.0)	120.8 (120.8)	120.7 (120.6)

<sup>a</sup> For numbering of the atoms see structure in the text. <sup>b</sup> Geometrical parameters optimized at the B3LYP/6-31+G(d) level are given in parentheses.

are directly estimated in experimental studies of the gas phase nucleophilic substitution reactions.<sup>29,30</sup>

We have found that  $\sigma$ -complex **3b** is a transition structure at both the HF/6-31+G(d) and B3LYP/6-31+G(d) levels (the imaginary frequency ( $b_1$ ) was calculated to be 501i and 323i  $\text{cm}^{-1}$ , respectively).  $\sigma$ -Complexes **3c** and **3d** are also predicted to be transition structures (the imaginary frequencies are 273i and 239i  $\text{cm}^{-1}$ , respectively, at the B3LYP/6-31+G(d) level, and 463i and 434i  $\text{cm}^{-1}$ , respectively, at the HF/6-31+G(d) level). These relatively high (in absolute value) imaginary frequencies make it hardly possible that the nature of the corresponding stationary points for **3b,3c** could change at a higher computational level. It is notable that the geometries of halobenzenes and  $\sigma$ -complexes **3b–d** optimized at the B3LYP/6-31+G(d) level are very close to those found by the MP2/6-31+G(d) optimization (Tables 2 and 3). The main difference is that the B3LYP/6-31+G(d) calculations lead to the slightly elongated C–X bond lengths in **1b–d** and **3b–d** as compared with the geometries optimized at the MP2/6-31+G(d) level, whereas the B3LYP calculated C–F bond lengths are shorter than those optimized at the MP2/6-31+G(d) level.

In contrast to complexes **3b–d**, the  $\sigma$ -complex **3a** of fluorobenzene with fluoride anion is a minimum both at the HF/6-31+G(d) and B3LYP/6-31+G(d) levels with the lowest frequency ( $b_1$ ) of 101 and 85  $\text{cm}^{-1}$ , respectively. For the  $\text{F}^- + \text{C}_6\text{H}_5\text{F}$  reaction, we have found that transition structure **4a** (Figure 2) has a higher energy (6.3  $\text{kJ mol}^{-1}$ ) than that of minimum **3a**. The C–F bond length in **4a** is only 0.011 Å longer when compared with the C–F bond in ion–molecule complex **2a** (Table 3). The distance between the attacking fluoride anion and the *ipso* carbon in **4a** is 1.870 Å (Figure 2), where the C–F bond lengths in  $\sigma$ -complex **3a** are 1.438 Å (Table 3). The FCF angle in transition structure **4a** (90.6°) is just slightly smaller than the FCF bond angle (94.8°) in  $\sigma$ -complex **3a**. The B3LYP/6-31+G(d) calculations lead to a similar geometry of transition structure **4a**. The main differences between the MP2 and B3LYP optimized geometries of **4a** are the distance between the attacking fluoride anion and the *ipso* carbon as well as the C–F bond length (Figure 2). The former is 0.294 Å longer at the B3LYP level than that at the MP2 level, whereas the latter is 0.032 Å shorter.

$\sigma$ -Complex **3a** and transition structure **4a** are 15.5 and 9.2  $\text{kJ mol}^{-1}$ , respectively, lower in energy than the

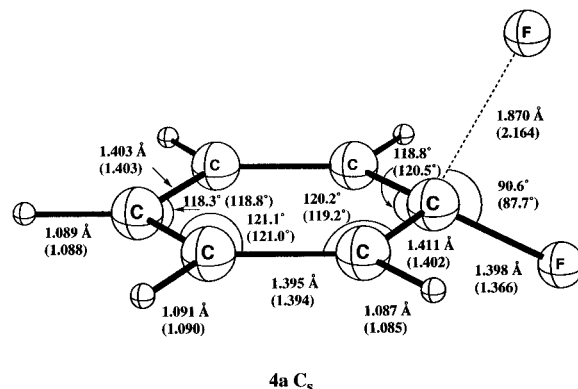


**Figure 2.** Geometry of the transition structure **4a** optimized at the MP2/6-31+G(d) and B3LYP/6-31+G(d) levels. The B3LYP-optimized geometrical parameters are shown in parentheses.

separated reactants, fluorobenzene **1a** and fluoride anion at the MP2/6-31+G(d) level (Table 1). The B3LYP calculated relative energies are slightly higher (Table 1). The relative energy of  $\sigma$ -complex **3a** with respect to loose ion–molecule complex **2a** is 55.6  $\text{kJ mol}^{-1}$  at the MP2/6-31+G(d) level (47.8  $\text{kJ mol}^{-1}$  at the B3LYP/6-31+G(d) level). The barrier for the isomerization of the  $\sigma$ -complex **3a** into the  $\text{FC}_6\text{H}_5\cdots\text{F}^-$  post-reaction ion–molecule complex is 6.3 and 11.3  $\text{kJ mol}^{-1}$  at the MP2/6-31+G(d) and B3LYP/6-31+G(d) levels, respectively. At the B3LYP/6-31+G(d) level, the relative energy of  $\sigma$ -complex **3a** with respect to the reactants is  $-26.8 \text{ kJ mol}^{-1}$ .

The negative overall barrier of  $-9.2 \text{ kJ mol}^{-1}$  for reaction (1) with X = F indicates that this reaction may be feasible in the gas phase provided that the other reaction processes do not dominate. In contrast, transition structures **3b–d** are considerably higher in energy (by 102.3 (Cl), 100.3 (Br), and 103.7 (I)  $\text{kJ mol}^{-1}$ )<sup>42</sup> than the isolated reactants and their overall barriers are higher (Table 1). Therefore, the magnitudes of these high overall barriers allow us to conclude that it would be unlikely to observe  $\text{S}_{\text{N}}\text{Ar}$  reactions (1) for X = Cl–I in the gas phase. It is notable that the overall barriers for X = Cl, Br, and I are very close each other. The similar

(42) MNDO calculations overestimate the stability of  $\sigma$ -complex **3b**. It is predicted to be a minimum lying only 29.7  $\text{kJ mol}^{-1}$  higher in energy than the isolated reactants. The overall barrier is calculated<sup>10a</sup> to be 49.0  $\text{kJ mol}^{-1}$ .

**Table 4. Values of  $A$  and %C–X Indexes Calculated for the  $\sigma$ -Complexes **3a–d** as well as the Experimental C–X Bond Dissociation Energies,  $D_0^{298}$  (in kJ mol<sup>-1</sup>),<sup>a</sup> for Halobenzenes **1a–d****

	$A^{b,c}$	%C–X <sup>c,d</sup>	exptl $D_0^{298}$
X = F ( <b>3a</b> )	0.939 (0.997) <sup>e</sup>	9.4	535.1 ± 4.2
X = Cl ( <b>3b</b> )	0.987 (1.000)	17.4	409.0 ± 3.8
X = Br ( <b>3c</b> )	0.997 (1.000)	19.4	346.2 ± 6.6
X = I ( <b>3d</b> )	0.999 (1.000)	20.6	281.6 ± 8.4

<sup>a</sup> Experimental estimates of the  $D_0(\text{C–X})$  values were obtained using the experimental enthalpies of formation ( $\Delta H_{f298}^\circ$ ) which were taken from ref 45 for halobenzenes, from ref 46 for the phenyl radical ( $339.7 \pm 2.5$  kJ mol<sup>-1</sup>), and from ref 37 for the halide anions. <sup>b</sup> See eq 6 in the text. <sup>c</sup> The  $A$  and %C–X indexes were calculated using the geometries optimized at the MP2/6-31+G(d) level. <sup>d</sup> Defined by eq 7, see the text. <sup>e</sup> The  $A$  index calculated for halobenzenes **1a–d** is shown in parentheses.

very small differences in the overall barrier heights have been found for the gas phase identity halogen-exchange reactions at saturated<sup>25</sup> and vinylic carbon.<sup>8</sup>

While the complexation energies calculated at the HF/6-31+G(d) + ZPE(HF/6-31+G(d)) level (60.9 (**2a**); 34.8 (**2b**); 30.6 (**2c**); 25.9 kJ mol<sup>-1</sup> (**2d**)) are only 10–15 kJ mol<sup>-1</sup> lower than those computed at the MP2/6-31+G(d) level of theory (Table 1), the overall and central barriers are much more sensitive to the level of theory. The  $\Delta H_{\text{ovr}}^\ddagger$  barriers calculated at the HF level (32.6 (F); 212.5 (Cl); 213.4 (Br); 216.7 kJ mol<sup>-1</sup> (I)) are about twice as great as the barriers found at the MP2 and B3LYP levels of theory. The HF/6-31+G(d) calculated central barriers (247.3 (Cl); 244.1 (Br); 242.6 kJ mol<sup>-1</sup> (I)) are about 100 kJ mol<sup>-1</sup> higher than the MP2/6-31+G(d)  $\Delta H_{\text{cent}}^\ddagger$  values (Table 1). This comparison of the barrier heights calculated at the HF and MP2 levels shows that reliable results can be obtained only if the correlation energy is taken into account. Results of a computational study of  $S_N\text{Ar}$  reactions at the HF level only may be very inaccurate.

Why is  $\sigma$ -complex **3a** a minimum, in contrast to analogous  $\sigma$ -complexes **3b–d** which correspond to first-order saddle points? One could consider the stability of  $\sigma$ -complexes **3** as governed by their aromatic stabilization which could still partially remain after the addition of the halide anion. It would suggest that the larger the aromatic character of the  $\sigma$ -complex **3**, the greater its stability. We estimated the aromaticity of **3a–d** using the  $A$  index<sup>43</sup> (eq 6):

$$A = 1 (225/n) \sum [(d_i - d_{\text{av}})/d_{\text{av}}]^2 \quad (6)$$

where  $d$  is the CC bond length (Å) in the benzene fragment having the  $n$  CC bonds ( $i = 1, \dots, n$ ) and  $d_{\text{av}}$  is the average value of all these  $n$  CC bond lengths. This index is one of structural criteria of aromaticity,<sup>44</sup> which are based on the estimation of the carbon–carbon bond length alternation in the arene ring. The aromatic character in  $\sigma$ -complexes **3b–d** is only slightly less than that in halobenzenes **1b–d** (Table 4). The  $A$  indexes show that structures **3b–d** retain a greater extent of

aromatic character than  $\sigma$ -complex **3a**. However, structures **3b–d** are not minima, whereas  $\sigma$ -complex **3a** is a minimum. Therefore, the extent of the aromatic stabilization of the  $\sigma$ -complexes **3** does not correlate with their stability. For **3b–d**, which are not minima, it is easier to restore the aromaticity by eliminating the halide anion than for the  $\sigma$ -complex **3a**, in which the formation of the second C–F bond significantly reduces the aromatic character of the arene moiety (Table 4).

The %C–X index (eq 7) yields an estimate of the C–X (X = F–I) bond length elongation in  $\sigma$ -complexes **3** as compared with the C–X bond length in **1**.

$$\%C-X = [R(\text{C-X})(\mathbf{3}) - R(\text{C-X})(\mathbf{1})]/R(\text{C-X})(\mathbf{1}) \times 100 \quad (7)$$

The values of the %C–X index for structures **3b–d**, which correspond to first-order saddle points, indicate that these structures possess rather loose C–X bonding, in contrast to  $\sigma$ -complex **3a** which is a minimum. The low polarizability of F as compared to other halogens results in its less repulsive interactions with such incoming small “hard” nucleophile as fluoride anion.<sup>3f</sup> In contrast, in the identity exchange  $S_N\text{Ar}$  reactions of the halobenzenes (X = Cl–I) with the “soft”, more polarizable halide anions, Cl<sup>-</sup>, Br<sup>-</sup>, and I<sup>-</sup>, the C–X bond formation occurs at larger distances (cf. the %C–X index values for **3b–d** and **3a**, Table 4). As a consequence, the barriers for X = Cl, Br, and I should not differ considerably and this agrees with the results of our calculations. Thus, the formation of the second C–X bond, which occurs at longer distances, does not significantly diminish the aromatic nature of the benzene moiety in **3b–d** and these structures transform without any barrier to the reactants or to the products with complete restoration of the aromatic system in the forming halobenzenes. In contrast to the concerted reactions (1) for X = Cl–I, a strong  $-I$  effect of *ipso* substituents such as fluorine stabilizes the  $\sigma$ -complex **3a**.<sup>3f,47</sup> In addition to this stabilization, a larger C–X bond energy for X = F (Table 4) results in much stronger C–F bonding in **3a** and the formation of the second C–F bond offsets the decrease in the aromatic character in **3a** when compared with **1a**. Therefore, we can conclude that the stronger the C–X bond, the greater tendency of the C<sub>6</sub>H<sub>5</sub>X<sub>2</sub><sup>-</sup>  $\sigma$ -complexes to be minima. In other words, if a nucleophile forms strong C–X bonds, it is possible that its identity exchange reaction<sup>48</sup> with an aromatic substrate will proceed via a multistep mechanism involving the formation of a stable  $\sigma$ -complex intermediate. The %C–X indexes demonstrate a linear correlation with the experimental C–X bond dissociation energies,  $D_0(\text{C–X})$  ( $r^2 = 0.942$ ; Table 4).

**Effect of Nitro Groups as Substituents on the Mechanism of the Gas Phase  $S_N\text{Ar}$  Reactions.** It is well-known that such electron-withdrawing substituents as the nitro group cause a considerable increase in reactivity in halogen-isotopic exchange  $S_N\text{Ar}$  reactions.<sup>2b,3f,49</sup> For example, while the  $S_N\text{Ar}$  reactions of unactivated chlorobenzene are very slow and could require elevated temperatures,<sup>2b</sup> the rate constants for chlorine-isotopic exchange for 1-chloro-2-nitrobenzene and 1-chloro-2,4-

(43) Jugl, A.; Francois, P. *Theoret. Chim. Acta* **1967**, *7*, 249.

(44) (a) Glukhovtsev, M. N. *J. Chem. Educ.* **1997**, *74*, 132. (b) Minkin, V. I.; Glukhovtsev, M. N.; Simkin, B. Ya. *Aromaticity and Antiaromaticity. Electronic and Structural Aspects*; Wiley: New York, 1994. (c) Glukhovtsev, M. N.; Simkin, B. Ya.; Minkin, V. I. *Russ. Chem. Rev.* **1985**, *54*, 54.

(45) Pedley, J. B.; Naylor, R. D.; Kirby, S. P. *Thermochemical Data of Organic Compounds*; Chapman and Hall: London, 1986.

(46) Davico, G. E.; Bierbaum, V. M.; DePuy, C. H.; Ellison, G. B.; Squires, R. S. *J. Am. Chem. Soc.* **1995**, *117*, 2590.

(47) (a) Bartoli, G.; Todesco, P. E. *Acc. Chem. Res.* **1977**, *10*, 125.

(b) Carey, F. A. *Organic Chemistry*; McGraw Hill: New York, 1987.

(48) We do not consider the nonidentity reactions with a different nucleophile and leaving group.

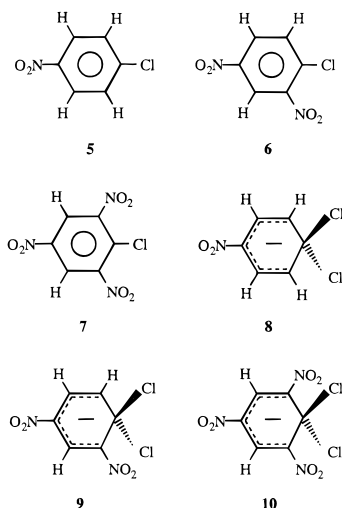
(49) Attia, M.; Dave, D.; Gore, P. H.; Ikejiani, A. O. O.; Morris, D. F. C.; Short, E. L. *J. Chem. Soc., Perkin Trans. 2* **1984**, 1637.

**Table 5. Total Energies and Zero-Point Energies of Halonitrobenzenes 5–7 and Their  $\sigma$ -Complexes with Chloride Anion 8–10 Calculated at the B3LYP/6-31+G(d) Level**

species	$E_{\text{tot}}^a$	ZPE <sup>b</sup>	NIMAG <sup>c</sup>
1-chloro-4-nitrobenzene <b>5</b> ( $C_s$ )	-896.364 159	245.5	0
1-chloro-2,4-dinitrobenzene <b>6</b> ( $C_1$ )	-1100.855 45	250.6	0
1-chloro-2,4,6-trinitrobenzene <b>7</b> ( $C_s$ )	-1305.342 066	255.4	0
$\sigma$ -complex ( <b>8</b> ) of <b>5</b> with chloride anion	-1356.630 36	241.9	1
$\sigma$ -complex ( <b>9</b> ) of <b>6</b> with chloride anion	-1561.149 118	249.3	0
$\sigma$ -complex ( <b>10</b> ) of <b>7</b> with chloride anion	-1765.658 77	255.4	0

<sup>a</sup> In hartrees. <sup>b</sup> In kJ mol<sup>-1</sup>, unscaled values. <sup>c</sup> Number of imaginary frequencies.

dinitrobenzene in sulfolane<sup>49</sup> at 313.2 K are  $7.25 \times 10^{-12}$  and  $3.1 \times 10^{-6}$ . In reactions with methoxide anion in methanol, 1-fluoro-2,4-dinitrobenzene is about  $10^3$  more reactive than 1-fluoro-4-nitrobenzene.<sup>2c</sup> The latter, in turn, is about  $10^7$  more reactive than fluorobenzene.<sup>2c</sup> A great accelerating effect of the nitro groups on the  $S_NAr$  reaction rate is explained by a presumption that the nitro group stabilizes not only the  $\sigma$ -complex itself<sup>50</sup> but the transition structure as well.<sup>3f</sup> Thus, we could expect that the introduction of nitro groups as substituents may result in a change in the reaction mechanism from a concerted to a multistep process involving the formation of a  $\sigma$ -complex intermediate.



Indeed, we have found that the  $\sigma$ -complexes **9** and **10** formed in the reactions of 1-chloro-2,4-dinitrobenzene (**6**) and picryl chloride (**7**) with chloride anion are minima at the B3LYP/6-31+G(d) level (Table 5). In contrast, the stabilizing effect of only one nitro group may not be strong enough to cause a qualitative change in the reaction mechanism. For example, although the existence of  $\sigma$ -complexes formed by trinitrobenzene and dinitrobenzene has been well established and many of them have been structurally characterized, no definitive data indicating the formation of such complexes involving mononitrobenzene have been reported to date.<sup>3f,15a</sup> We have found that this  $\sigma$ -complex is only a shallow minimum at the HF/6-31+G(d) level (the lowest frequency is only 41 cm<sup>-1</sup>) and corresponds a well-defined transition structure (Figure 3) at the B3LYP/6-31+G(d) level (the imaginary frequency is 202i cm<sup>-1</sup>). A remarkable result is that although the nitro group in **5** cannot stabilize the  $\sigma$ -complex as a minimum, the stabilizing effect of this

(50) It should be noted that the mesomeric effect of nitro group, which is often invoked to explain a role of the nitro group as a substituent, is very small in nitrobenzenes, in contrast to the inductive effect.<sup>51</sup>

(51) Exner, O.; Krygowski, T. M. *Acc. Chem. Res.* **1996**, *29*, 71.

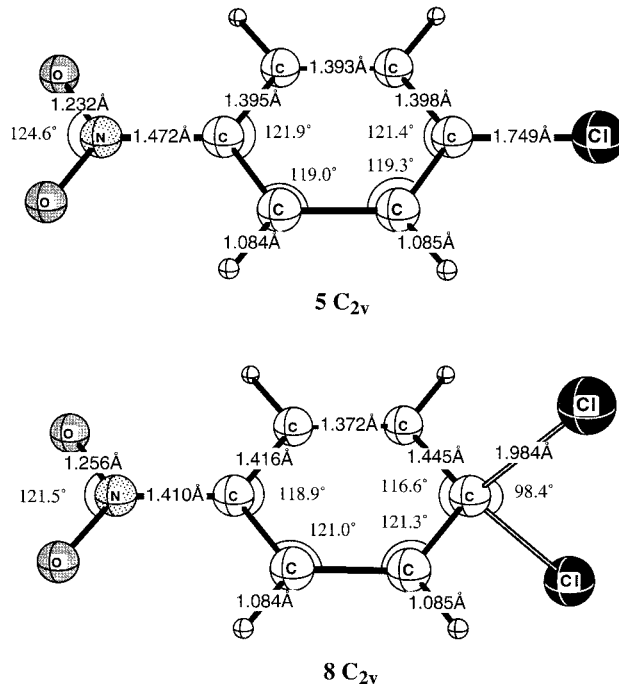
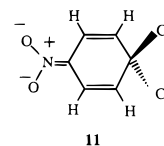


**Figure 3.** Geometries of 1-chloro-4-nitrobenzene (**5**) and its  $\sigma$ -complex (**8**) with chloride anion optimized at the B3LYP/6-31+G(d) level.

substituent on the  $\sigma$ -complex is reflected in a much smaller overall barrier for the anion exchange (18.6 kJ mol<sup>-1</sup>) (Table 6). This suggests that the  $O_2NC_6H_4Cl$  (**5**) +  $Cl^-$   $S_NAr$  reaction is feasible in the gas phase, in contrast to the reactions (1) of the unactivated halobenzenes. The  $\sigma$ -complexes **9** and **10** (Figures 4 and 5) are 51.4 and 110.4 kJ mol<sup>-1</sup> lower in energy than the separated reactants (Table 6). This suggests that the overall barriers may be low (or perhaps negative).



In agreement with the X-ray data on 1-chloro-2,4-dinitrobenzene (**6**),<sup>52</sup> our calculations show that the nitro groups in **6** are not coplanar with the aromatic ring (Figure 4). A nonplanar arrangement of the nitro group was also found for **7** where the CCNO dihedral angles are even larger than those in **6** (Figure 4). In contrast, the nitro groups are coplanar to the arene ring in  $\sigma$ -complexes **9** and **10** (Figures 4 and 5). The cyclohexadienylidene ring has a planar geometry in  $\sigma$ -complexes **7–10**. The C–N bond lengths in  $\sigma$ -complexes **8–10** are shorter than those in the reactants **5–7**. The C–N bond

(52) Watson, K. J. *Nature* **1960**, *188*, 1102.



**Table 6. Energies of the  $\sigma$ -Complexes **3b** and **8–10** with Respect to the Isolated Reactants ( $\Delta H_{\text{ovr}}$ ) For Halogen-Exchange Identity  $S_{\text{N}}\text{Ar}$  Reactions of Chlorobenzene **1b** and Chloronitrobenzenes **5–8** With Chloride Anion and the Stabilization Energies (SE) of  $\sigma$ -Complexes **3b** and **8–10** Calculated at the B3LYP/6-31+G(d) + ZPE(B3LYP/6-31+G(d)) Computational Level**

reactions	$\Delta H_{\text{ovr}}^a$	SE <sup>a,b</sup>	%C–Cl <sup>c</sup>
chlorobenzene <b>1a</b> + Cl <sup>−</sup>	112.7	0	20.9
1-chloro-4-nitrobenzene ( <b>5</b> ) + Cl <sup>−</sup>	18.6	94.1	13.4
1-chloro-2,4-dinitrobenzene ( <b>6</b> ) + Cl <sup>−</sup>	−51.4	164.1	10.2
1-chloro-2,4,6-trinitrobenzene ( <b>7</b> ) + Cl <sup>−</sup>	−110.4	223.0	8.9

<sup>a</sup>  $\Delta H_{\text{ovr}}$  and SE are in kJ mol<sup>−1</sup>. <sup>b</sup> The SE values are the enthalpies of reactions (8). <sup>c</sup> %C–Cl are calculated for  $\sigma$ -complexes **3b** and **8–10** using the equation similar to eq 7.

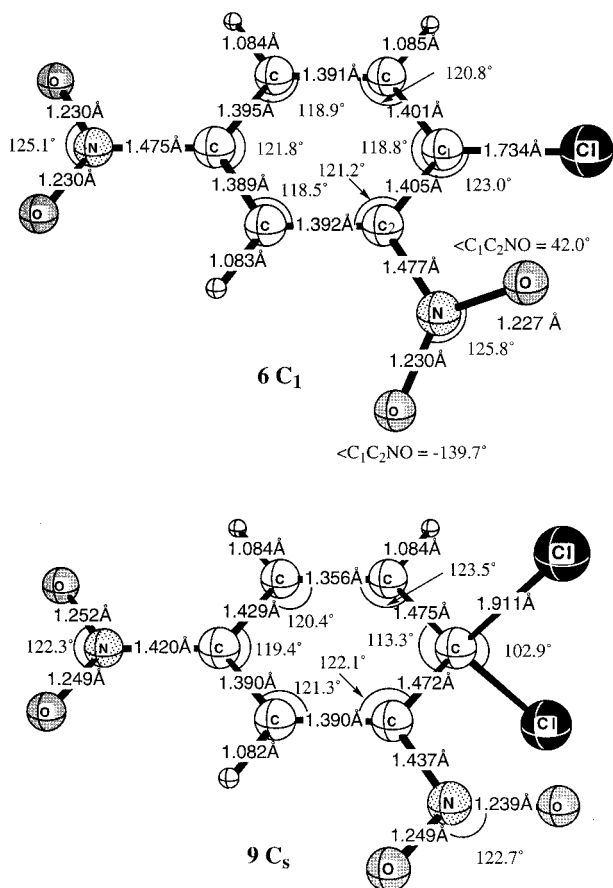


**Figure 4.** Geometries of 1-chloro-2,4-dinitrobenzene (**6**) and its  $\sigma$ -complex (**9**) with chloride anion optimized at the B3LYP/6-31+G(d) level.

length for the *p*-nitro group in **8–10** is shortened by 0.062, 0.055, and 0.049 Å, respectively, when compared with that in **5–7**. While these C–N bond lengths in chloronitrobenzenes **5–7** (1.472 Å (**5**); 1.475 Å (**6**); 1.477 Å (**7**)) calculated at the B3LYP/6-31+G(d) level are very close to the C–N bond length in nitromethane (1.489 Å, microwave spectroscopy),<sup>53</sup> the shorter C–N bond lengths for the *p*-nitro group in  $\sigma$ -complexes **8–10** (1.410 (**8**); 1.420 (**9**); 1.428 Å (**10**)) can possibly reflect the mesomeric effect of the nitro group enforced by strong electron-donating properties of the anionic moiety in **8–10**. This effect can result in a partial double-bond character of these C–N bonds. A similar short C–N bond length has been found in the X-ray study on *p*-nitrophenolate anion (1.418 Å).<sup>54</sup> While the C–N bond lengths in  $\sigma$ -complexes **8–10** are shortened with an increasing of the number of

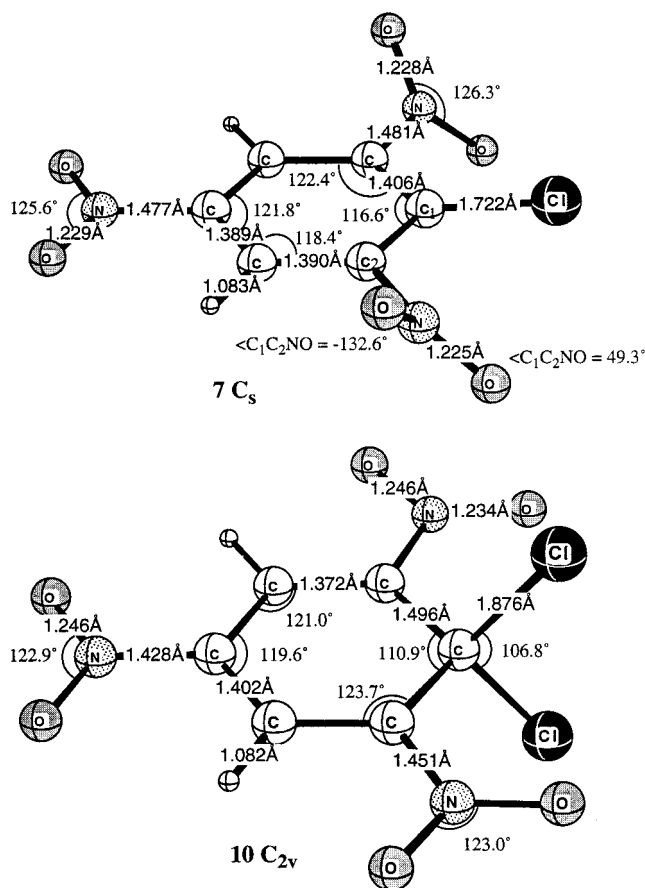


**Figure 5.** Geometries of 1-chloro-2,4,6-trinitrobenzene (**7**) and its  $\sigma$ -complex (**10**) with chloride anion optimized at the B3LYP/6-31+G(d) level.

nitro groups, the O–N bonds are elongated as compared with those in chloronitrobenzenes **5–7** (e.g., for the *p*-nitro group: 1.232 (**5**)/1.256 Å (**8**); 1.230 (**6**)/1.252 and 1.249 Å (**9**); 1.229 (**7**)/1.246 Å (**10**)). This can also be considered as a geometrical manifestation of the mesomeric effect of the nitro groups in the  $\sigma$ -complexes **8–10** (see, for example, the canonical structure **11**), whereas this effect is considerably diminished in nitrobenzenes lacking electron-donating substituents.<sup>51</sup>

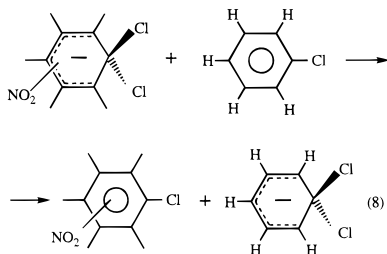
The differences in the C–N and O–N bond lengths for the *o*-NO<sub>2</sub> group in  $\sigma$ -complexes **9** and **10** and the reactants **6** and **7** are less than those for the *p*-nitro groups. This agrees with a much stronger capability of a *p*-versus an *o*-nitro group to withdraw electrons by means of the mesomeric effect and to stabilize  $\sigma$ -complexes.<sup>3f,6a</sup> The twisted arrangements of the *o*-NO<sub>2</sub> group in chloro-2,4-dinitrobenzene **6** and chloro picrate **7** (Figures 4 and 5) would suggest that the C–N bond lengths in these groups should differ considerably from those in a *p*-NO<sub>2</sub> group having a planar geometry when compared with the differences in  $\sigma$ -complexes **9** and **10**

(53) Cox, A. P.; Waring, S. J. *J. Chem. Soc., Faraday Trans. 2* **1972**, *68*, 1060.

(54) Krygowski, T. M.; Turowska-Tyrk, I. *Collect. Czech. Chem. Commun.* **1990**, *55*, 165.

in which all the nitro groups possess a planar bond configuration. It is notable, however, that in contrast to these expectations, the C–N bond length differences between the *o*-NO<sub>2</sub> group and *p*-NO<sub>2</sub> group are much smaller in chloronitrobenzenes **6** and **7** (0.002 and 0.004 Å, respectively) than those between such groups in  $\sigma$ -complexes **9** and **10** (0.040 and 0.030 Å, respectively) where the mesomeric effect which is different for *o*-NO<sub>2</sub> and *p*-NO<sub>2</sub> groups, operates. The C–N bond lengths calculated for  $\sigma$ -complex **10** (1.428, 1.451, and 1.451 Å) are close to those found by X-ray studies of 1,1-dimethoxy-2,4,6-trinitrocyclohexadienylide (1.387, 1.456, and 1.439 Å, respectively).<sup>55</sup> Whereas the Cl–C–Cl bond angle widens from 93.3° for **3b** (Table 3) to 106.8° for **10** (Figure 5), the C–C(*ipso*)–C bond angle decreases from 119.1° for **3b** to 110.9° for **10**. The C–C(*ipso*) bond lengths increase from 1.411 Å for **3b** (Table 3) to 1.445 Å for **8** to 1.496 Å for **10**. These changes in the C–C(*ipso*)–C bond angle and the C–C(*ipso*) bond lengths reflect the changes in the hybridization of the *ipso* carbon from sp<sup>2</sup>-type to sp<sup>3</sup>-type.

The electron-withdrawing effect of the nitro groups is reflected in the charges calculated using natural population analysis (NPA)<sup>56</sup> at the B3LYP/6-31+G(d) level. The group charges for *o*- and *p*-NO<sub>2</sub> groups in **10** are –0.354 and –0.410, respectively. The arene moiety in **10** bears a positive group charge of +0.222. In contrast, the arene group charge in **8** is –0.021 and the NPA group charge of the NO<sub>2</sub> group is –0.523. The oxygen atoms in **8** have negative charges of –0.492, whereas the charge at the nitrogen is +0.461 (see canonical structure **11**). The large electron-withdrawing effect of the three nitro groups in **10** results in significantly smaller (in absolute value) charges at the chlorines in **10** (–0.052) than those in **8** (–0.228).



The stabilization energies<sup>57</sup> for  $\sigma$ -complexes **8–10** calculated at the B3LYP/6-31+G(d) + ZPE(B3LYP/6-31+G(d)) level as the enthalpies of the reaction (8) show that the introduction of the first nitro group leads to a stabilization of 94.1 kJ mol<sup>–1</sup> and the second and third nitro groups bring the additional stabilization of the  $\sigma$ -complex by 70.0 and 128.9 kJ mol<sup>–1</sup>, respectively (Table 6). The introduction of nitro groups into the chlorobenzene cycle causes a decrease of the %C–Cl index calculated for the  $\sigma$ -complexes **3b** and **8–10** vs substrates **1b** and **5–7** (Table 6), from 20.9 for **3b/1b** to 8.9% for **10/7**. The smaller %C–Cl indexes reflect the stronger C–Cl bonding. These indexes display linear correlations with

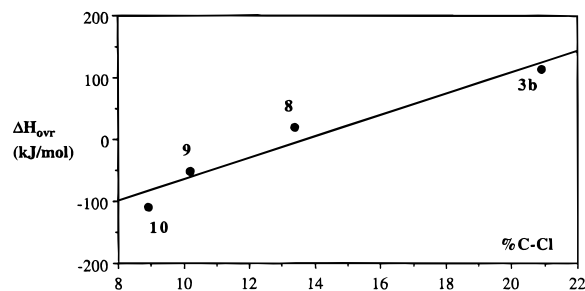


**Figure 6.** Plot of the energy differences ( $\Delta H_{ovr}$ ) between the  $\sigma$ -complexes **3b** and **8–10** formed in the gas phase chloride-exchange  $S_NAr$  reactions of chlorobenzene **1b** and chloronitrobenzenes **5–7** and the isolated reactants vs the %C–Cl indexes for these  $\sigma$ -complexes. The  $\Delta H_{ovr}$  and %C–Cl values are listed in Table 6.

the stabilization energies, SE ( $r^2 = 0.945$ ; the smaller %C–Cl value, the larger SE value) and with the energy differences between the  $\sigma$ -complexes and the isolated reactants,  $\Delta H_{ovr}$  ( $r^2 = 0.945$ ; Figure 6). These energy differences and the stabilization energies correlate each other by their definitions.

#### 4. Conclusions

(1) The  $C_6H_5X + X^-$  ( $X = Cl-I$ )  $S_NAr$  reactions proceed without the formation of a stable  $C_6H_5X_2^-$   $\sigma$ -complex intermediate. The overall barriers of these reactions in which the  $C_{2v}$  structures of  $C_6H_5X_2^-$  ( $X = Cl-I$ ) are transition structures are 102.3 (Cl), 100.3 (Br), and 103.7 (I) kJ mol<sup>–1</sup> at the MP2/6-31+G(d) level. The calculations at the B3LYP/6-31+G(d) level lead to similar barrier heights of 112.7, 111.7, and 113.6 kJ mol<sup>–1</sup>, respectively. The barriers vary in a small range of just 2–3 kJ mol<sup>–1</sup> and do not exhibit any clear dependence on the nature of halogen. The high overall barriers allow us to conclude that it would be unlikely to observe the  $S_NAr$  reactions (1) for  $X = Cl-I$  in the gas phase.

(2) While the  $S_NAr$  reaction of 1-chloro-4-nitrobenzene with chloride anion also proceeds via a concerted mechanism, the stabilizing effect of the nitro group on the  $O_2NC_6H_4Cl_2^-$   $\sigma$ -complex **8** leads to an overall barrier which is only 18.6 kJ mol<sup>–1</sup> with respect to the isolated reactants calculated at the B3LYP/6-31+G(d) + ZPE(B3LYP/6-31+G(d)) level. This suggests that this reaction may be feasible in the gas phase, in contrast to the  $C_6H_5X + X^-$  ( $X = Cl-I$ )  $S_NAr$  reactions of the unactivated halobenzenes.

(3) The stabilization energies for  $\sigma$ -complexes **8–10** formed in the reactions of 1-chloro-4-nitrobenzene (**5**), 1-chloro-2,4-dinitrobenzene (**6**), and picryl chloride (**7**) with chloride anion demonstrate that the introduction of the first nitro group leads to a stabilization of 94.1 kJ mol<sup>–1</sup> and the second and third nitro groups bring an additional stabilization of 70.0 and 128.9 kJ mol<sup>–1</sup>, respectively (at the B3LYP/6-31+G(d) + ZPE(B3LYP/6-31+G(d)) level). As a consequence, the gas phase reactions of the 1-chloro-2,4-dinitrobenzene (**6**) and picryl chloride (**7**) with chloride anion follow a multistep mechanism with the formation of the  $\sigma$ -complexes **9** and **10** as intermediates.

(4) The  $C_6H_5F + F^-$   $S_NAr$  reaction follows a multistep mechanism with the formation of a discrete  $C_6H_5F_2^-$   $\sigma$ -complex intermediate, the energy of which is 15.5 kJ mol<sup>–1</sup> lower than that of the isolated reactants. The activation barrier for the elimination of the fluoride anion

(55) Ueda, H.; Sakabe, N.; Tanaka, J.; Furusaki, A. *Bull. Chem. Soc. Jpn.* **1968**, *41*, 2866.

(56) (a) Reed, A. E.; Weinstock, R. B.; Weinhold, F. *J. Chem. Phys.* **1985**, *83*, 735. (b) Reed, A. E.; Curtiss, L. A.; Weinhold, F. *Chem. Rev.* **1988**, *88*, 899. (c) Weinhold, F.; Carpenter, J. E. In *The Structure of Small Molecules and Ions*; Naaman, R., Vager, Z., Eds.; Plenum Press: New York, 1988; p 227. (d) Reed, A. E.; Weinhold, F. *Israel J. Chem.* **1991**, *31*, 277.

(57) Birch, A. J.; Hinde, A. L.; Radom, L. *J. Am. Chem. Soc.* **1980**, *102*, 6430.

from this complex is  $6.3 \text{ kJ mol}^{-1}$  at the MP2/6-31+G(d) + ZPE(HF/6-31+G(d)) level. The negative overall barrier of  $-9.2 \text{ kJ mol}^{-1}$  for reaction (1) with  $X = \text{F}$  indicates that this reaction may be feasible in the gas phase provided that alternative reactions do not dominate.

(5) The stronger the C–X bond and the greater the electronegativity of X, the greater tendency for the  $\text{C}_6\text{H}_5\text{X}_2^-$   $\sigma$ -complexes to be minima. In other words, if a nucleophile forms a strong C–X bond, it is possible that its identity exchange  $\text{S}_{\text{N}}\text{Ar}$  reaction with an aromatic substrate proceeds via a multistep mechanism involving the formation of a  $\sigma$ -complex as an intermediate.

(6) The ion–molecule complex  $\text{F}^- \cdots \text{C}_6\text{H}_5\text{F}$  has the largest complexation energy ( $71.1 \text{ kJ mol}^{-1}$ ), whereas the complexation energies for  $\text{X}^- \cdots \text{C}_6\text{H}_5\text{X}$  ( $X = \text{Cl-I}$ ) vary in a range of  $10 \text{ kJ mol}^{-1}$ , from  $48.9$  (Cl) to  $38.4$  (I)  $\text{kJ mol}^{-1}$ . The complexation energies for the  $\text{X}^- \cdots \text{C}_6\text{H}_5\text{X}$  ( $X = \text{F-I}$ ) complexes are close to those for  $\text{X}^- \cdots \text{H}_3\text{CX}$  ( $X = \text{F-I}$ ) and  $\text{X}^- \cdots \text{H}_2\text{C}=\text{CHX}$  ( $X = \text{F-I}$ ) ion–molecule complexes formed in the gas phase reactions of methyl halide and vinyl halide, respectively, with halide anions. The complexation energies for methyl and vinyl halides are similar in magnitude to the complexation energies of  $\text{X}^- \cdots \text{C}_6\text{H}_5\text{X}$  ( $X = \text{F-I}$ ), which demonstrate good linear correlations with Mulliken ( $r^2 = 0.985$ ) and Pauling ( $r^2 = 0.993$ ) electronegativities of the halogens.

(7) The calculations on the  $\text{C}_6\text{H}_5\text{X} + \text{X}^-$  ( $X = \text{F-I}$ )  $\text{S}_{\text{N}}\text{-Ar}$  reactions at the MP2 and B3LYP levels lead to close

values of their complexation energies, overall and central barriers. The correlation energy has to be taken into account in the calculations of the overall and central barriers in the gas phase  $\text{S}_{\text{N}}\text{Ar}$  reactions. Results of a computational study of  $\text{S}_{\text{N}}\text{Ar}$  reactions at the Hartree–Fock level only may be very inaccurate.

**Acknowledgment.** This work has been supported by the National Science Foundation (CHE-9531242) and Molten Metal Technology. We thank National Center for Supercomputing Applications (Urbana, IL) and Pittsburgh Supercomputing Center for allocation of computer time. M.N.G. also thanks Dr. N. J. R. van Eikema Hommes (Erlangen, Germany) for making available the Molecule program which was used to prepare Figures 2–5.

**Supporting Information Available:** Total energies and zero point energies (in  $\text{kJ mol}^{-1}$ ) of the reactants and products, ion–molecule complexes, transition structures for  $\text{S}_{\text{N}}\text{Ar}$  reactions (1) calculated at the HF/6-31+G(d), MP2/6-31+G(d), and B3LYP/6-31+G(d) levels; structures of ion–molecule complexes **2a–d** optimized at the MP2/6-31+G(d) level (2 pages). This material is contained in libraries on microfiche, immediately follows this article in the microfilm version of the journal, and can be ordered from the ACS; see any current masthead page for ordering information.

JO962096E